

ISSN 1726-5479

SENSORS & TRANSDUCERS

vol. 116
5 / 10



Sensor Buses and Interfaces

International Frequency Sensor Association Publishing



Editors-in-Chief: professor Sergey Y. Yurish, tel.: +34 696067716, fax: +34 93 4011989, e-mail: editor@sensorsportal.com

Editors for Western Europe

Meijer, Gerard C.M., Delft University of Technology, The Netherlands
Ferrari, Vittorio, Università di Brescia, Italy

Editor South America

Costa-Felix, Rodrigo, Inmetro, Brazil

Editor for Eastern Europe

Sachenko, Anatoly, Ternopil State Economic University, Ukraine

Editors for North America

Datskos, Panos G., Oak Ridge National Laboratory, USA
Fabien, J. Josse, Marquette University, USA
Katz, Evgeny, Clarkson University, USA

Editor for Asia

Ohyama, Shinji, Tokyo Institute of Technology, Japan

Editor for Asia-Pacific

Mukhopadhyay, Subhas, Massey University, New Zealand

Editorial Advisory Board

- Abdul Rahim, Ruzairi**, Universiti Teknologi, Malaysia
Ahmad, Mohd Noor, Northern University of Engineering, Malaysia
Annamalai, Karthigeyan, National Institute of Advanced Industrial Science and Technology, Japan
Arcega, Francisco, University of Zaragoza, Spain
Arguel, Philippe, CNRS, France
Ahn, Jae-Young, Korea Institute of Science and Technology, Korea
Arndt, Michael, Robert Bosch GmbH, Germany
Ascoli, Giorgio, George Mason University, USA
Atalay, Selcuk, Inonu University, Turkey
Atghiaee, Ahmad, University of Tehran, Iran
Augutis, Vygantas, Kaunas University of Technology, Lithuania
Avachit, Patil Lalchand, North Maharashtra University, India
Ayesh, Aladdin, De Montfort University, UK
Bahreyni, Behraad, University of Manitoba, Canada
Baliga, Shankar, B., General Motors Transnational, USA
Baoxian, Ye, Zhengzhou University, China
Barford, Lee, Agilent Laboratories, USA
Barlingay, Ravindra, RF Arrays Systems, India
Basu, Sukumar, Jadavpur University, India
Beck, Stephen, University of Sheffield, UK
Ben Bouzid, Sihem, Institut National de Recherche Scientifique, Tunisia
Benachaiba, Chellali, Universitaire de Bechar, Algeria
Binnie, T. David, Napier University, UK
Bischoff, Gerlinde, Inst. Analytical Chemistry, Germany
Bodas, Dhananjay, IMTEK, Germany
Borges Carval, Nuno, Universidade de Aveiro, Portugal
Bousbia-Salah, Mounir, University of Annaba, Algeria
Bouvet, Marcel, CNRS – UPMC, France
Brudzewski, Kazimierz, Warsaw University of Technology, Poland
Cai, Chenxin, Nanjing Normal University, China
Cai, Qingyun, Hunan University, China
Campanella, Luigi, University La Sapienza, Italy
Carvalho, Vitor, Minho University, Portugal
Cecelja, Franjo, Brunel University, London, UK
Cerda Belmonte, Judith, Imperial College London, UK
Chakrabarty, Chandan Kumar, Universiti Tenaga Nasional, Malaysia
Chakravorty, Dipankar, Association for the Cultivation of Science, India
Changhai, Ru, Harbin Engineering University, China
Chaudhari, Gajanan, Shri Shivaji Science College, India
Chavali, Murthy, VIT University, Tamil Nadu, India
Chen, Jiming, Zhejiang University, China
Chen, Rongshun, National Tsing Hua University, Taiwan
Cheng, Kuo-Sheng, National Cheng Kung University, Taiwan
Chiang, Jeffrey (Cheng-Ta), Industrial Technol. Research Institute, Taiwan
Chiriac, Horia, National Institute of Research and Development, Romania
Chowdhuri, Arijit, University of Delhi, India
Chung, Wen-Yaw, Chung Yuan Christian University, Taiwan
Corres, Jesus, Universidad Publica de Navarra, Spain
Cortes, Camilo A., Universidad Nacional de Colombia, Colombia
Courtois, Christian, Université de Valenciennes, France
Cusano, Andrea, University of Sannio, Italy
D'Amico, Arnaldo, Università di Tor Vergata, Italy
De Stefano, Luca, Institute for Microelectronics and Microsystem, Italy
Deshmukh, Kiran, Shri Shivaji Mahavidyalaya, Barshi, India
Dickert, Franz L., Vienna University, Austria
Dieguez, Angel, University of Barcelona, Spain
Dimitropoulos, Panos, University of Thessaly, Greece
Ding, Jianning, Jiangsu Polytechnic University, China
Kim, Min Young, Kyungpook National University, Korea South
Djordjevic, Alexandar, City University of Hong Kong, Hong Kong
Donato, Nicola, University of Messina, Italy
Donato, Patricio, Universidad de Mar del Plata, Argentina
Dong, Feng, Tianjin University, China
Drljaca, Predrag, Instersema Sensoric SA, Switzerland
Dubey, Venketesh, Bournemouth University, UK
Enderle, Stefan, Univ. of Ulm and KTB Mechatronics GmbH, Germany
Erdem, Gursan K. Arzum, Ege University, Turkey
Erkmen, Aydan M., Middle East Technical University, Turkey
Estelle, Patrice, Insa Rennes, France
Estrada, Horacio, University of North Carolina, USA
Faiz, Adil, INSA Lyon, France
Fericean, Sorin, Balluff GmbH, Germany
Fernandes, Joana M., University of Porto, Portugal
Francioso, Luca, CNR-IMM Institute for Microelectronics and Microsystems, Italy
Francis, Laurent, University Catholique de Louvain, Belgium
Fu, Weiling, South-Western Hospital, Chongqing, China
Gaura, Elena, Coventry University, UK
Geng, Yanfeng, China University of Petroleum, China
Gole, James, Georgia Institute of Technology, USA
Gong, Hao, National University of Singapore, Singapore
Gonzalez de la Rosa, Juan Jose, University of Cadiz, Spain
Granell, Annette, Goteborg University, Sweden
Graff, Mason, The University of Texas at Arlington, USA
Guan, Shan, Eastman Kodak, USA
Guillet, Bruno, University of Caen, France
Guo, Zhen, New Jersey Institute of Technology, USA
Gupta, Narendra Kumar, Napier University, UK
Hadjiloucas, Sillas, The University of Reading, UK
Haider, Mohammad R., Sonoma State University, USA
Hashsham, Syed, Michigan State University, USA
Hasni, Abdelhafid, Bechar University, Algeria
Hernandez, Alvaro, University of Alcalá, Spain
Hernandez, Wilmar, Universidad Politecnica de Madrid, Spain
Homentcovschi, Dorel, SUNY Binghamton, USA
Horstman, Tom, U.S. Automation Group, LLC, USA
Hsiai, Tzung (John), University of Southern California, USA
Huang, Jeng-Sheng, Chung Yuan Christian University, Taiwan
Huang, Star, National Tsing Hua University, Taiwan
Huang, Wei, PSG Design Center, USA
Hui, David, University of New Orleans, USA
Jaffrezic-Renault, Nicole, Ecole Centrale de Lyon, France
Jaime Calvo-Galleg, Jaime, Universidad de Salamanca, Spain
James, Daniel, Griffith University, Australia
Janting, Jakob, DELTA Danish Electronics, Denmark
Jiang, Liudi, University of Southampton, UK
Jiang, Wei, University of Virginia, USA
Jiao, Zheng, Shanghai University, China
John, Joachim, IMEC, Belgium
Kalach, Andrew, Voronezh Institute of Ministry of Interior, Russia
Kang, Moonho, Sunmoon University, Korea South
Kaniusas, Eugenijus, Vienna University of Technology, Austria
Katake, Anup, Texas A&M University, USA
Kausel, Wilfried, University of Music, Vienna, Austria
Kavasoglu, Nese, Mugla University, Turkey
Ke, Cathy, Tyndall National Institute, Ireland
Khan, Asif, Aligarh Muslim University, Aligarh, India
Sapozhnikova, Ksenia, D.I.Mendeleyev Institute for Metrology, Russia
Saxena, Vibha, Bhabha Atomic Research Centre, Mumbai, India

Ko, Sang Choon, Electronics. and Telecom. Research Inst., Korea South
Kockar, Hakan, Balikesir University, Turkey
Kotulska, Malgorzata, Wroclaw University of Technology, Poland
Kratz, Henrik, Uppsala University, Sweden
Kumar, Arun, University of South Florida, USA
Kumar, Subodh, National Physical Laboratory, India
Kung, Chih-Hsien, Chang-Jung Christian University, Taiwan
Lacnjevac, Caslav, University of Belgrade, Serbia
Lay-Ekuakille, Aime, University of Lecce, Italy
Lee, Jang Myung, Pusan National University, Korea South
Lee, Jun Su, Amkor Technology, Inc. South Korea
Lei, Hua, National Starch and Chemical Company, USA
Li, Genxi, Nanjing University, China
Li, Hui, Shanghai Jiaotong University, China
Li, Xian-Fang, Central South University, China
Liang, Yuanchang, University of Washington, USA
Liawruangrath, Saisunee, Chiang Mai University, Thailand
Liew, Kim Meow, City University of Hong Kong, Hong Kong
Lin, Hermann, National Kaohsiung University, Taiwan
Lin, Paul, Cleveland State University, USA
Linderholm, Pontus, EPFL - Microsystems Laboratory, Switzerland
Liu, Aihua, University of Oklahoma, USA
Liu Changgeng, Louisiana State University, USA
Liu, Cheng-Hsien, National Tsing Hua University, Taiwan
Liu, Songqin, Southeast University, China
Lodeiro, Carlos, University of Vigo, Spain
Lorenzo, Maria Encarnacio, Universidad Autonoma de Madrid, Spain
Lukaszewicz, Jerzy Pawel, Nicholas Copernicus University, Poland
Ma, Zhanfang, Northeast Normal University, China
Majstorovic, Vidosav, University of Belgrade, Serbia
Marquez, Alfredo, Centro de Investigacion en Materiales Avanzados, Mexico
Matay, Ladislav, Slovak Academy of Sciences, Slovakia
Mathur, Prafull, National Physical Laboratory, India
Maurya, D.K., Institute of Materials Research and Engineering, Singapore
Mekid, Samir, University of Manchester, UK
Melnyk, Ivan, Photon Control Inc., Canada
Mendes, Paulo, University of Minho, Portugal
Mennell, Julie, Northumbria University, UK
Mi, Bin, Boston Scientific Corporation, USA
Minas, Graca, University of Minho, Portugal
Moghavvemi, Mahmoud, University of Malaya, Malaysia
Mohammadi, Mohammad-Reza, University of Cambridge, UK
Molina Flores, Esteban, Benemérita Universidad Autónoma de Puebla, Mexico
Moradi, Majid, University of Kerman, Iran
Morello, Rosario, University "Mediterranea" of Reggio Calabria, Italy
Mounir, Ben Ali, University of Sousse, Tunisia
Mulla, Imtiaz Sirajuddin, National Chemical Laboratory, Pune, India
Neelamegam, Periasamy, Sastra Deemed University, India
Neshkova, Milka, Bulgarian Academy of Sciences, Bulgaria
Oberhammer, Joachim, Royal Institute of Technology, Sweden
Ould Lahoucine, Cherif, University of Guelma, Algeria
Pamidighanta, Sayanu, Bharat Electronics Limited (BEL), India
Pan, Jisheng, Institute of Materials Research & Engineering, Singapore
Park, Joon-Shik, Korea Electronics Technology Institute, Korea South
Penza, Michele, ENEA C.R., Italy
Pereira, Jose Miguel, Instituto Politecnico de Setebal, Portugal
Petsev, Dimiter, University of New Mexico, USA
Pogacnik, Lea, University of Ljubljana, Slovenia
Post, Michael, National Research Council, Canada
Prance, Robert, University of Sussex, UK
Prasad, Ambika, Gulbarga University, India
Prateepasen, Asa, Kingmoungut's University of Technology, Thailand
Pullini, Daniele, Centro Ricerche FIAT, Italy
Pumera, Martin, National Institute for Materials Science, Japan
Radhakrishnan, S., National Chemical Laboratory, Pune, India
Rajanna, K., Indian Institute of Science, India
Ramadan, Qasem, Institute of Microelectronics, Singapore
Rao, Basuthkar, Tata Inst. of Fundamental Research, India
Raouf, Kosai, Joseph Fourier University of Grenoble, France
Reig, Candid, University of Valencia, Spain
Restivo, Maria Teresa, University of Porto, Portugal
Robert, Michel, University Henri Poincare, France
Rezazadeh, Ghader, Urmia University, Iran
Royo, Santiago, Universitat Politecnica de Catalunya, Spain
Rodriguez, Angel, Universidad Politecnica de Cataluna, Spain
Rothberg, Steve, Loughborough University, UK
Sadana, Ajit, University of Mississippi, USA
Sadeghian Marnani, Hamed, TU Delft, The Netherlands
Sandacci, Serghei, Sensor Technology Ltd., UK
Schneider, John K., Ultra-Scan Corporation, USA
Seif, Selemani, Alabama A & M University, USA
Seifter, Achim, Los Alamos National Laboratory, USA
Sengupta, Deepak, Advance Bio-Photonics, India
Shah, Kriyang, La Trobe University, Australia
Shearwood, Christopher, Nanyang Technological University, Singapore
Shin, Kyuho, Samsung Advanced Institute of Technology, Korea
Shmaliy, Yuriy, Kharkiv National Univ. of Radio Electronics, Ukraine
Silva Girao, Pedro, Technical University of Lisbon, Portugal
Singh, V. R., National Physical Laboratory, India
Slomovitz, Daniel, UTE, Uruguay
Smith, Martin, Open University, UK
Soleymampour, Ahmad, Damghan Basic Science University, Iran
Somani, Prakash R., Centre for Materials for Electronics Technol., India
Srinivas, Talabattula, Indian Institute of Science, Bangalore, India
Srivastava, Arvind K., Northwestern University, USA
Stefan-van Staden, Raluca-Ioana, University of Pretoria, South Africa
Sumriddetchka, Sarun, National Electronics and Computer Technology Center, Thailand
Sun, Chengliang, Polytechnic University, Hong-Kong
Sun, Dongming, Jilin University, China
Sun, Junhua, Beijing University of Aeronautics and Astronautics, China
Sun, Zhiqiang, Central South University, China
Suri, C. Raman, Institute of Microbial Technology, India
Sysoev, Victor, Saratov State Technical University, Russia
Szewczyk, Roman, Industrial Research Inst. for Automation and Measurement, Poland
Tan, Ooi Kiang, Nanyang Technological University, Singapore
Tang, Dianping, Southwest University, China
Tang, Jaw-Luen, National Chung Cheng University, Taiwan
Teker, Kasif, Frostburg State University, USA
Thumbavanam Pad, Kartik, Carnegie Mellon University, USA
Tian, Gui Yun, University of Newcastle, UK
Tsiantos, Vassilios, Technological Educational Institute of Kaval. Greece
Tsigara, Anna, National Hellenic Research Foundation, Greece
Twomey, Karen, University College Cork, Ireland
Valente, Antonio, University, Vila Real, - U.T.A.D., Portugal
Vanga, Raghav Rao, Summit Technology Services, Inc., USA
Vaseashta, Ashok, Marshall University, USA
Vazquez, Carmen, Carlos III University in Madrid, Spain
Vieira, Manuela, Instituto Superior de Engenharia de Lisboa, Portugal
Vigna, Benedetto, STMicroelectronics, Italy
Vrba, Radimir, Brno University of Technology, Czech Republic
Wandelt, Barbara, Technical University of Lodz, Poland
Wang, Jiangping, Xi'an Shiyou University, China
Wang, Kedong, Beihang University, China
Wang, Liang, Pacific Northwest National Laboratory, USA
Wang, Mi, University of Leeds, UK
Wang, Shinn-Fwu, Ching Yun University, Taiwan
Wang, Wei-Chih, University of Washington, USA
Wang, Wensheng, University of Pennsylvania, USA
Watson, Steven, Center for NanoSpace Technologies Inc., USA
Weiping, Yan, Dalian University of Technology, China
Wells, Stephen, Southern Company Services, USA
Wolkenberg, Andrzej, Institute of Electron Technology, Poland
Woods, R. Clive, Louisiana State University, USA
Wu, DerHo, National Pingtung Univ. of Science and Technology, Taiwan
Wu, Zhaoyang, Hunan University, China
Xiu Tao, Ge, Chuzhou University, China
Xu, Lisheng, The Chinese University of Hong Kong, Hong Kong
Xu, Tao, University of California, Irvine, USA
Yang, Dongfang, National Research Council, Canada
Yang, Wuqiang, The University of Manchester, UK
Yang, Xiaoling, University of Georgia, Athens, GA, USA
Yaping Dan, Harvard University, USA
Ymeti, Aurel, University of Twente, Netherland
Yong Zhao, Northeastern University, China
Yu, Haihu, Wuhan University of Technology, China
Yuan, Yong, Massey University, New Zealand
Yufera Garcia, Alberto, Seville University, Spain
Zakaria, Zulkarnay, University Malaysia Perlis, Malaysia
Zagnoni, Michele, University of Southampton, UK
Zamani, Cyrus, Universitat de Barcelona, Spain
Zeni, Luigi, Second University of Naples, Italy
Zhang, Minglong, Shanghai University, China
Zhang, Quintao, University of California at Berkeley, USA
Zhang, Weiping, Shanghai Jiao Tong University, China
Zhang, Wenming, Shanghai Jiao Tong University, China
Zhang, Xueji, World Precision Instruments, Inc., USA
Zhong, Haoxiang, Henan Normal University, China
Zhu, Qing, Fujifilm Dimatix, Inc., USA
Zorzano, Luis, Universidad de La Rioja, Spain
Zourab, Mohammed, University of Cambridge, UK

Contents

Volume 116
Issue 5
May 2010

www.sensorsportal.com

ISSN 1726-5479

Research Articles

- Composite Cavity Fiber Laser for Sensor Applications**
Asrul Izam Azmi, Ian Leung, Paul Childs and Gang-Ding Peng 1
- Design, Development and Testing of a Semi Cylindrical Capacitive Sensor for Liquid Level Measurement**
Sagarika Pal, Rasmiprava Barik..... 13
- Humidity Sensitivity of MgCr₂O₄-TiO₂-LiO₂ Ceramics Sensor Prepared by Sol-Gel Routes**
H. Y. He 21
- Effect on Ethanol Gas Sensing Performance of Cu Addition to TiO₂ Thick Films**
C. G. Dighavkar, A. V. Patil, S. J. Patil and R. Y. Borse 28
- Feasibility of Passive Gas Sensor Based on Whispering Gallery Modes and its RADAR Interrogation: Theoretical and Experimental Investigations**
Hamida Hallil, Franck Chebila, Philippe Menini and Hervé Aubert 38
- Simulation-Driven Development and Optimization of a High-Performance Six-Dimensional Wrist Force/Torque Sensor**
Qiaokang Liang, Dan Zhang, Quanjun Song and Yunjian Ge 49
- Kalman Smoothing and Wavelet Analysis for Inertial Data of Human Movement Disorder Motion**
Wesley Teskey, Mohamed Elhabiby and Naser El-Sheimy 61
- Two-Phase Flow Regime Identification by Ultrasonic Computerized Tomography**
Mohd Hafiz Fazalul Rahiman, Ruzairi Abdul Rahim, Jaysuman Pusppanathan 76
- Approximations in Calculating Stray Capacitance of Printed Spiral Inductors**
R. C. Woods 83
- Harmonic Response of Magneto-electro-elastic Sensors Bonded to Cylindrical Shells**
B. Biju, N. Ganesan and K. Shankar 89
- Ultra High Voltage Surge Waveforms Measurement Using an Optical Transducer**
Francisco G. Peña-Lecona, J. Muñoz-Maciel, G. Gómez-Rosas, Francisco J. Casillas-Rodríguez, M. Mora-González, Víctor M. Durán-Ramírez and C. Castillo-Quevedo 104
- Transverse Micro-structuring of Photonic Crystal Fibers for Industrial Sensors and Side Viewing Probes for Optical Coherence Tomography Applications**
Sanjay Kher, Manoj Kumar Saxena, Smita Chaube, Amit Keskar, Subhashish Tiwari, S. M. Oak... 112
- Stability of High Temperature Standard Platinum Resistance Thermometers at High Temperatures**
Y. A. Abdelaziz and F. M. Megahed..... 122

Authors are encouraged to submit article in MS Word (doc) and Acrobat (pdf) formats by e-mail: editor@sensorsportal.com
Please visit journal's webpage with preparation instructions: http://www.sensorsportal.com/HTML/DIGEST/Submission.htm

International Frequency Sensor Association (IFSA).

IFSA SENSORS WEB PORTAL
 Primary Internet Resource for **SENSORS**,
 100% Target Audience

TURN OUR VISITORS INTO YOUR CUSTOMERS BY THE SHORTEST WAY

<http://www.sensorsportal.com/HTML/Sensor.htm>
sales@sensorsportal.com

MEDIA KIT 2010

NanoSEE 08
Nano materials industrial Status and Expected Evolution

UNIQUE REPORT DESCRIBING NANO MATERIAL WORLD UP TO 2012

This report is designed to understand the market for nanomaterials, the players including the organizations, as well as the accessibility of the market. It highlights the technical functions made possible by nanomaterials to create our daily nanoproducts.

Reports answer to:

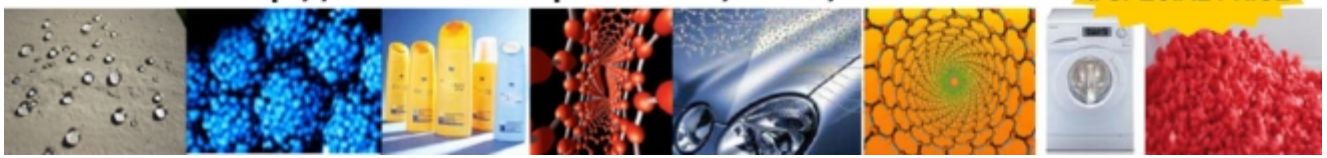
- What are nanomaterials? What are they used for?
- What are the benefits of nanomaterials?
- What is the market for nanomaterials - 2007-2012?
- Who are the key players? How is the industry organized?

Unique proposition selling

- Complete overview of the nanomaterials world: products, players, applications, markets...
- Understanding the industrial value chain

<http://www.sensorsportal.com/HTML/NanoSEE.htm>

IFSA offers a SPECIAL PRICE



Composite Cavity Fiber Laser for Sensor Applications

Asrul Izam AZMI, Ian LEUNG, Paul CHILDS and Gang-Ding PENG

School of Electrical Engineering and Telecommunications,

The University of New South Wales, Australia

Tel.: +61293855411, fax: +61293855993

E-mail: asrul@student.unsw.edu.au

Received: 25 March 2010 /Accepted: 24 May 2010 /Published: 31 May 2010

Abstract: Composite Cavity Fiber Lasers (CCFLs) are investigated for their potential in sensing applications. We have theoretically studied the frequency and intensity related sensing characteristics of CCFLs. A CCFL can be fabricated simply by writing three wavelength-matched Bragg gratings directly into a continuous length of doped fiber. Using an in-house grating writing facility we have fabricated CCFLs of varying composite cavity lengths. We have simulated and experimentally examined the sensing capabilities of CCFLs under different strain conditions, and found that CCFLs give rise to significantly distinctive responses from those of a FBG or single cavity fiber laser based sensor. We also noted significant intensity and / or frequency (wavelength) responses under different loading conditions, thus making them suitable for intensity or frequency-based sensing. A particular example of application is to use an asymmetrically strained CCFL to achieve increased sensitivity, decreased gauge length, and very confined spectral requirements. *Copyright © 2010 IFSA.*

Keywords: Composite cavity fiber laser, Strain sensor, Long cavity, Dual cavity laser

1. Introduction

Fiber lasers have made considerable advances in numerous applications, including the fields of sensing, telecommunications and high power lasers. Among the many successful utilizations of fiber lasers for sensing are the detection of pressure [1, 2], temperature [3, 4], and gas [5, 6]. There are several key advantages of optical fiber based devices compared to their electronic counterparts; such that optical fiber devices are more compact, lighter, electrically passive and immune to electromagnetic interference (EMI). Since there is no 'electronic end', they tend to be more robust when deployed in harsh environments where electronic devices may be prone to failure such as

underwater applications. The costs of packaging therefore can be reduced without affecting reliability. Fiber lasers are particularly interesting for sensing because of their enhanced sensitivity due to cavity resonance, improved signal to noise ratio due to higher signal power and their narrower linewidth. Furthermore, fiber laser fabrication processes are now well developed, relatively straightforward and cost effective with good accuracy and repeatability. Fiber lasers have been deployed as an interrogation source [7, 8] or as a sensing head itself [1, 2, 9, 10], where some schemes have demonstrated comparable performances to conventional electronic sensors such as the interferometric based sensor [11]. Several configurations of fiber laser strain sensors (which are normally classified based on the type of perturbation induced on the optical signal by the measurand), such as intensity, wavelength or phase and polarization, have been studied. As opposed to lasers for telecommunications, fiber lasers as sensing elements are designed to be very susceptible to one, or several, particular external perturbation(s).

In this report, Composite Cavity Fiber Lasers (CCFLs) are investigated theoretically and experimentally for their sensitivity enhancement. The CCFL is distinguished from the single cavity laser by an additional third reflector which provides self feedback to the main cavity. The purpose of the feedback was previously demonstrated in semiconductor laser for linewidth narrowing [12, 13], low frequency wavelength fluctuations [14] and continuous wavelength tuning [15, 16]. However, for our case of fiber sensing purpose, the feedback modifies the phase and gain condition, which subsequently changes the intensity and spectral response of the laser. One particular point of interest of the CCFL based sensor is that, when one cavity is made nonresponsive, significant intensity or/and frequency response can be observed. Such characteristics could be very useful in intensity or/and wavelength based sensing in various applications such as pressure, strain and acoustic sensing. In Sections 2 and 3, we present an analytical model to examine the phase and gain condition, and sensing characteristics of CCFL. In Sections 4 and 5, we present experiment results that evaluate the spectral, intensity and sensing performance of the long cavity CCFLs designed and fabricated in house. We consistently used similar CCFL throughout the experiment with dimension of $L_1=3$ cm and $L_2=9$ cm (3 cm / 9 cm) where L_1 and L_2 are the cavity lengths between successive reflectors.

2. CCFL: Phase and Gain Conditions

A CCFL is simply made up of three wavelengths matched FBGs written in a continuous length of erbium doped fiber (EDF) is illustrated in Fig. 1.

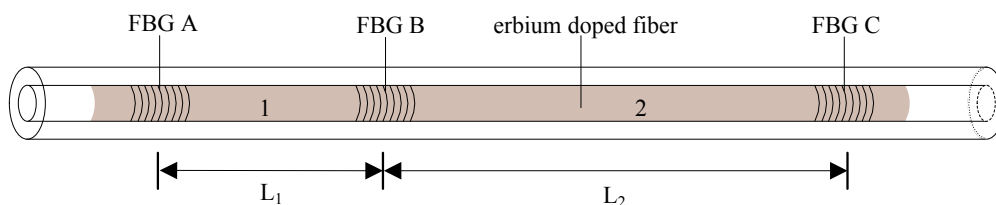


Fig. 1. Novel Composite Cavity Fiber Laser with an active internal feedback.

A brief explanation of the theoretical analysis applied to solve the boundary value problem for the fields in the CCFL is given below, which is similar to the approaches given in [17, 18]. Taking into consideration the effects of multiple reflections of the composite cavity structure, the potential of net optical gain in both cavities and the symmetrical properties of an FBG, the general condition for the phase and gain conditions for the CCFL can be written as [19]:

$$r_A r_B e^{i\phi_1} g_1 + r_B r_C e^{i\phi_2} g_2 + (1 - 2r_B^2) r_A r_C e^{i(\phi_1 + \phi_2)} g_1 g_2 = 1, \quad (1)$$

where r_A , r_B and r_C are the amplitude reflection coefficients for FBGs A, B and C respectively. For simplicity, the FBGs are assumed to be very short (not spatially distributed) with rectangular reflection profiles (uniform reflectivity within its reflection band). $\phi_j = 2k_j L_j$ and $g_j = e^{2(\gamma_j - \alpha_j)L_j}$, ($j = 1$ and 2) represent the round trip phase and gain respectively for the corresponding sub-cavity, k_j is the propagation constant, L_j is the length of the sub-cavity and γ_j and α_j are the linear gain and absorption coefficients per unit length respectively. Equation (1) for the CCFL is significantly different to its counterpart for the traditional semiconductor external cavity laser, and gives rise to different results. In the following analysis, L_1 is considered the primary cavity, and a complex feedback parameter z is defined as:

$$z = \frac{1 - r_B r_C e^{i\phi_2} g_2}{1 + (1 - 2r_B^2) \frac{r_C}{r_B} e^{i\phi_2} g_2}, \quad (2)$$

Equation (1) can be further written as:

$$g_1 = \frac{e^{-i\phi_1}}{r_A r_B} z = \frac{e^{-i\phi_1}}{r_A r_B} e^{G_z + i\phi_z} = e^{2(\gamma_1 - \alpha_1)L_1}, \quad (3)$$

where $G_z = \ln|z|$ and $\phi_z = \angle z$ are related to the magnitude and phase of z respectively. From Equation (3), the gain and phase conditions of the CCFL can be derived by separating the real and imaginary terms and are given by:

$$2\gamma_{1\text{threshold}} L_1 = 2\alpha_1 L_1 - \ln(r_A r_B) + G_z, \quad (4)$$

$$\phi_z - \phi_1 = p2\pi, \quad p \text{ integer}, \quad (5)$$

In Equation (4), G_z is an additive term of the threshold gain which differentiate it from Fabry-Perot laser. Equation (5) is wavelength dependant via the propagation constant, $k = 2\pi/(n\lambda)$ with n being the effective refractive index of the doped fiber. It is apparent that the left hand side (LHS) of (5) is a periodic function with period determined by n_2 and L_2 , while right hand side (RHS) of (5) is a set of near linear equations with slope controlled by n_1 and L_1 . Any change of either L_1 or L_2 (due to sensing) will change the slope of the RHS of (5) or the period of the LHS of (5) respectively. Hence, the locations of the intersections of these equations will change from the original condition, resulting in a change in the lasing response of the CCFL.

3. Sensing Characteristics

When a uniform strain (or pressure) field is applied to the total length of the CCFL, its wavelength response is similar to the typical FBG sensor or single cavity fiber laser. However, when the sub-cavities of the CCFL sensor experience a dissimilar strain field (e.g. by packaging with materials of different Young's Modulus), different responses are expected. This partial straining concept is illustrated in Fig. 2, where only one sub-cavity is mechanically strained while another sub-cavity is mechanically isolated.

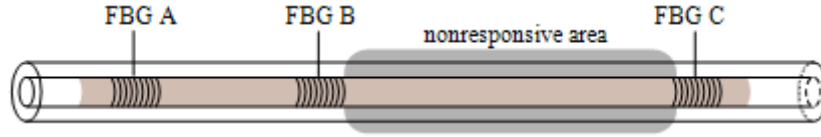


Fig. 2. The shaded area of the CCFL indicate the cavity area that is mechanically isolated to realize the partial cavity sensing, while other parts are used for sensing.

While equations (1) to (5) are general, we limit our case analysis to the CCFLs we have fabricated and tested. To investigate the differences in sensing response between total and partial straining of the CCFL, the numerical values used for the following simulations are $r_B=0.8$, $r_{Cg2}=0.7$, $n=1.456$ and sub-cavity lengths of (3 cm, 9 cm). It is necessary to mention that different sub-cavity lengths combinations will result different sensitivity characteristics. However it will be shown later, at a particular sub-cavity length dimension, the sensitivity can be optimized by the feedback parameter, represented by r_{Cg2} . The selection of the (3 cm, 9 cm) dimension is to demonstrate that by having long total cavity length, the CCFL can operate in a single longitudinal mode, thus realizing a coherent output with higher power. Furthermore, it shows that the flexibility of operating CCFL sensor by adjustment of pump power and hence the gain (g_2), to achieve certain sensitivity level. Fig. 3 and 4, shows the results for ϕ_z and G_z under various straining conditions. Here the wavelength range is selected in agreement with the wavelength and spectral width of the Bragg reflectors of the CCFLs. The ϕ_z plot is a graphical interpretation of the phase matching condition of Equation (5) (the LHS of (5) is plotted as a solid line, and the RHS as a dashed line), where the intersections indicate wavelengths which satisfy the phase condition. G_z is plotted separately, with an X marking the wavelengths where the phase matching condition is satisfied.

3.1. Zero CCFL Straining

The results for ϕ_z and G_z for the zero strain condition are indicated in Fig. 3. When the 3cm sub-cavity is considered the primary sub-cavity, two longitudinal modes exist. On the other hand, if the 9cm sub-cavity is considered the primary cavity, three additional modes with positive G_z are identified over the same wavelength range. However, due to the self-injection-type interaction within the CCFL, these additional modes will be suppressed during operation. The following investigation will consider the case where the 3cm sub-cavity is the primary cavity.

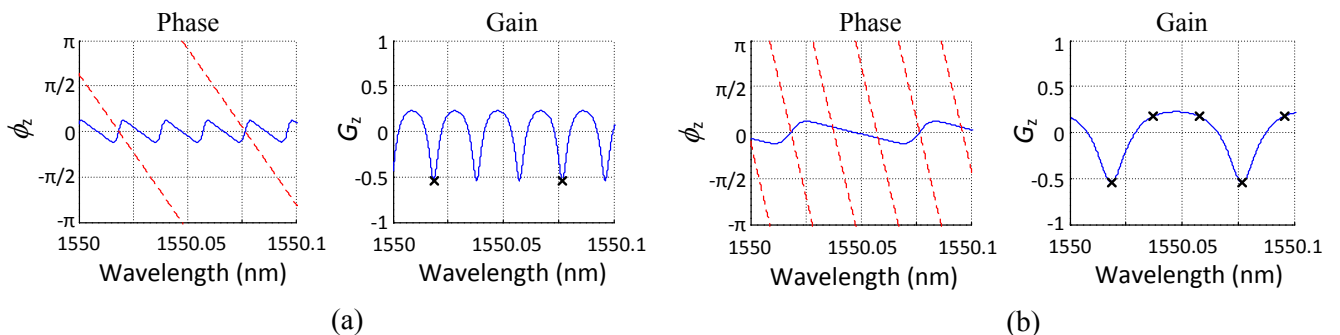


Fig. 3. Phase and gain adjustment for the zero strain condition of a CCFL with (a) a 3 cm long primary sub-cavity and a 9 cm long secondary sub-cavity and (b) a 9 cm long primary sub-cavity and a 3 cm long secondary sub-cavity.

3.2. Total and Partial CCFL Straining

For the total straining case, both sub-cavities of the CCFL experience the same strain (as such the length ratio $L_2:L_1$ remains the same) and therefore both sides of (5) shift by the same amount. In this case, even though the wavelengths which satisfy the phase condition have shifted due to the applied strain, as shown in Fig. 4(a), the relative position of the intersections with respect to ϕ_z and the corresponding values of G_z remain unchanged. However, the length ratio does alter when the two sub-cavities of the CCFL are strained separately. The phase matching condition shown in Fig. 4(b) represents the case when only the secondary sub-cavity is strained, where only LHS of (5) has shifted. Alternatively, when only the primary sub-cavity is strained, as shown in Fig. 4(c), only the dashed line corresponding to the RHS of (5) is affected.

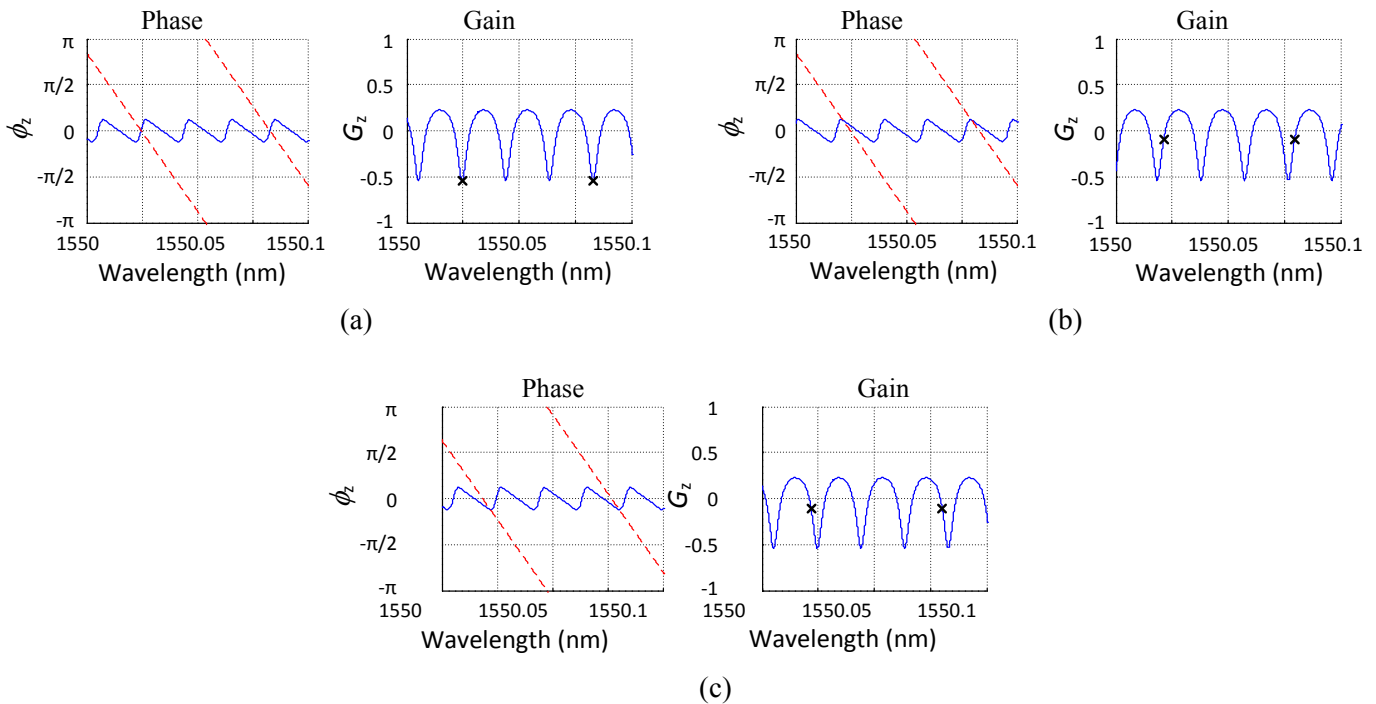


Fig. 4. Phase and gain adjustment with longitudinal load $4\mu\epsilon$ for (a) total CCFL straining to both (3 cm and 9 cm) sub-cavities; (b) partial CCFL straining to the 9 cm sub-cavity; and (c) partial CCFL straining to the 3 cm sub-cavity.

3.3. Sensitivity Comparison

Although the same amount of strain ($4\mu\epsilon$) was applied in the results shown in Fig. 4(a) to 4(c), the observed wavelength shift differed between the three straining formats. This variation in sensitivity is related to the amplitude of ϕ_z , so that when the LHS and RHS of (5) scanned across each other due to strain, the wavelength-value of the intersections also changed at a different rate. Embodied in Fig. 5 are the wavelength and G_z responses to strain of the three straining formats. For the total CCFL straining format, its wavelength response is linear and no change is expected in G_z . By adjusting the results with a scaling factor of 0.78 when taking into consideration of the stress-optical effect of silica, the wavelength response is approximately $1.17\text{ pm}/\mu\epsilon$. These results show that under the total CCFL straining format, a CCFL strain sensor behaves the same as other typical FBG based sensors [20]. For the two partial CCFL sensing formats, the wavelength response is nonlinear. For the case which involves straining only the primary sub-cavity, alternating sections of faster and slower wavelength

response can be observed. If a substantial amount of strain is applied, the response follows that of the total CCFL straining format. For dynamic small-signal sensing applications such as acoustic sensing, applying a pre-strain, or similarly provide a phase shift, in order to bias (in this case, $6 \mu\epsilon$) the CCFL allows it to operate at a wavelength with higher sensitivity. For the case which involves straining only the secondary sub-cavity, the lasing wavelength oscillates (alternating sections of positive and negative responses) between a confined range. Differing from the other partial straining format, the wavelength shift remains negligible when a substantial amount of strain is applied. However, with adequate fringe counting methods, this straining format can be applied for sensing, and allows for higher multiplexing capacity due to the smaller wavelength allocation requirement. Apart from the distinctive non-linear wavelength response, the partial straining formats will also induce changes in G_z with strain. In Fig. 5(b), the response of G_z for both partial CCFL straining formats is identical, and the sensitivity is maximized at strain values that correspond to the ‘elbows’ of the wavelength response. Since G_z is regarded as an additive term that alters the threshold gain, partial straining of the CCFL should lead to changes in output intensity. Such an attribute should cause partially strained CCFL sensors to be preferential in low cost and highly robust intensity-based sensing systems.

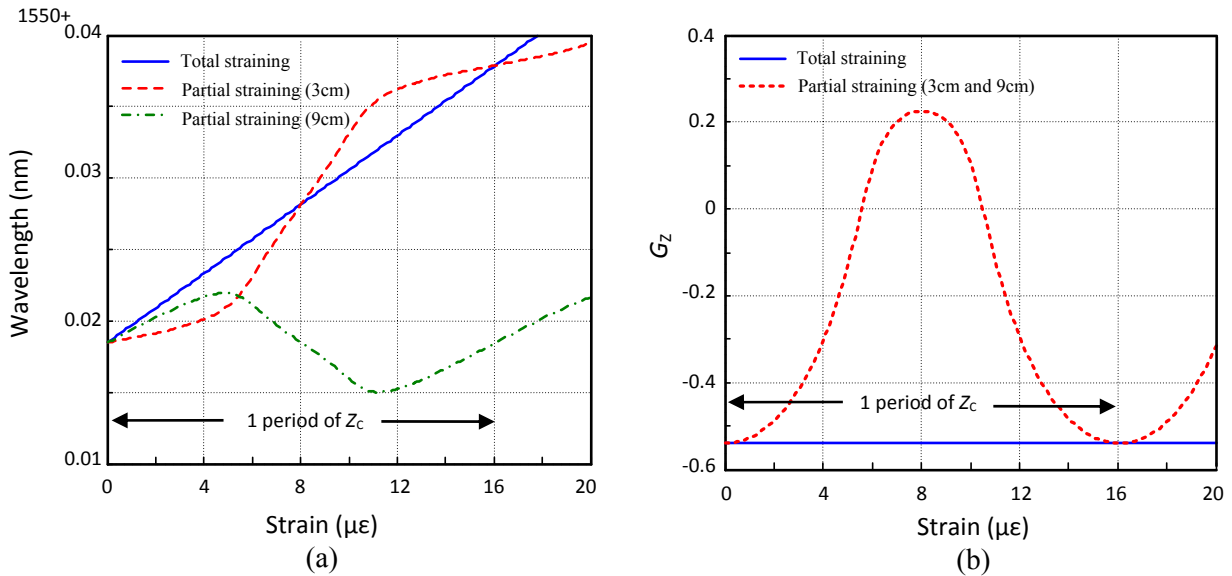


Fig. 5. Results of the three different sensing formats for (a) wavelength response; and (b) G_z response.

3.4. Maximum Sensitivity

As indicated previously, the varying sensitivity of the partial CCFL straining formats are related to the amplitude of ϕ_z , as the locus of z follows a circular path in the complex plane. The size of the locus of z is in turn related to r_B and r_{Cg2} . Depicted in Fig. 6 is the maximum sensitivity of the three straining formats. These results are specific to the condition $r_B = 0.8$. When only the 3cm primary sub-cavity is strained, feedback from the secondary sub-cavity caused the sensitivity to reach as much as 2.6 times higher than that of the total CCFL straining format. On the other hand, if the secondary sub-cavity is strained, higher sensitivity than that of the total CCFL straining format is also possible, but only within the range of $0.75 < r_{Cg2} < 4.75$. These results show that the control of r_{Cg2} (from the grating strength and amount of pumping power during operation) is crucial in determining the sensitivity improvements.

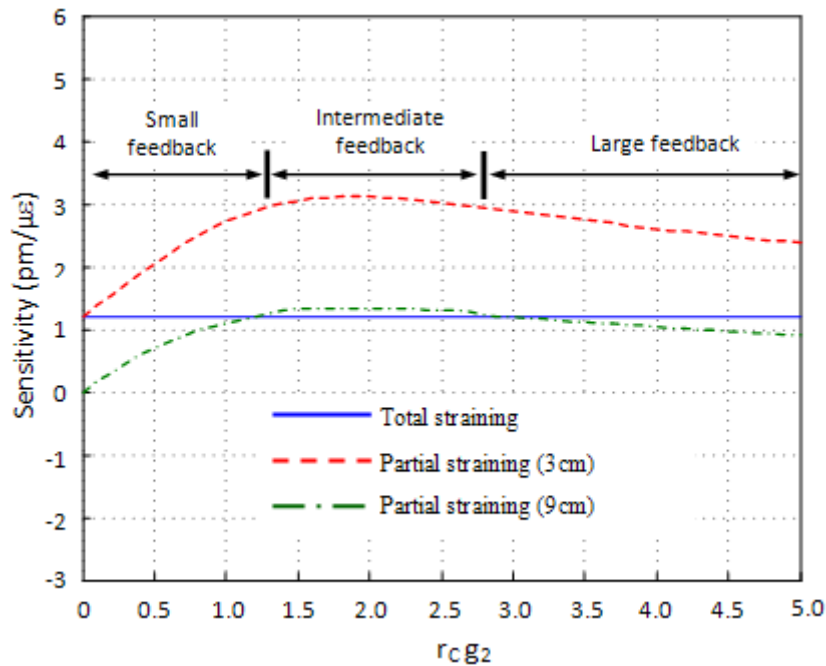


Fig. 6. Maximum sensitivity comparison between total and partial CCFL straining.

4. Fabrication and Characterizations of CCFL

4.1. Fabrication of CCFL

To demonstrate the ability of the CCFL design to produce long cavity length lasers having a single longitudinal mode, passive spectral of a CCFL used for in the experiment is presented. The CCFL was fabricated by a scanning UV side exposure technique with a phase mask. It was fabricated at the center of the EDF, such that the unoccupied lengths of EDF are the same on either end. No apodization was applied when writing each of the 6 mm FBGs. Measurements at each stage of the writing process were taken using a tunable scanning laser. As indicated by Fig. 7, the EDF used for writing has approximately 5 dB transmission loss which is attributed to the absorption of the EDF and coupling loss due to the splices between different fiber types. After FBG A was written, a typically smooth and symmetric loss profile can be observed. The FBG has a 3 dB width of 0.15 nm, and provides -10 dB loss at the Bragg wavelength, which is equivalent to approximately 90 % power reflection, or an amplitude reflectivity of 0.95. Due to the high repeatability of the writing system, gratings with same properties of FBG A (such as reflectivity, spectral width and central wavelength) are expected. The second FBG to be written was FBG-B, after which fine, and mostly symmetric, modal details in the order of the free spectral range of a 2 cm Fabry Perot cavity can be observed. When all three FBGs were written, the passive modal structure becomes even more complicated due to the establishment of the 8cm cavity. The roughly 0.3 nm shift in the structure's wavelength at the final stage is caused by the relaxation of the pre-strain applied during the writing process. The measured transmission loss and relative consistency of the bandwidth throughout indicates that the three FBGs are spectrally matched.

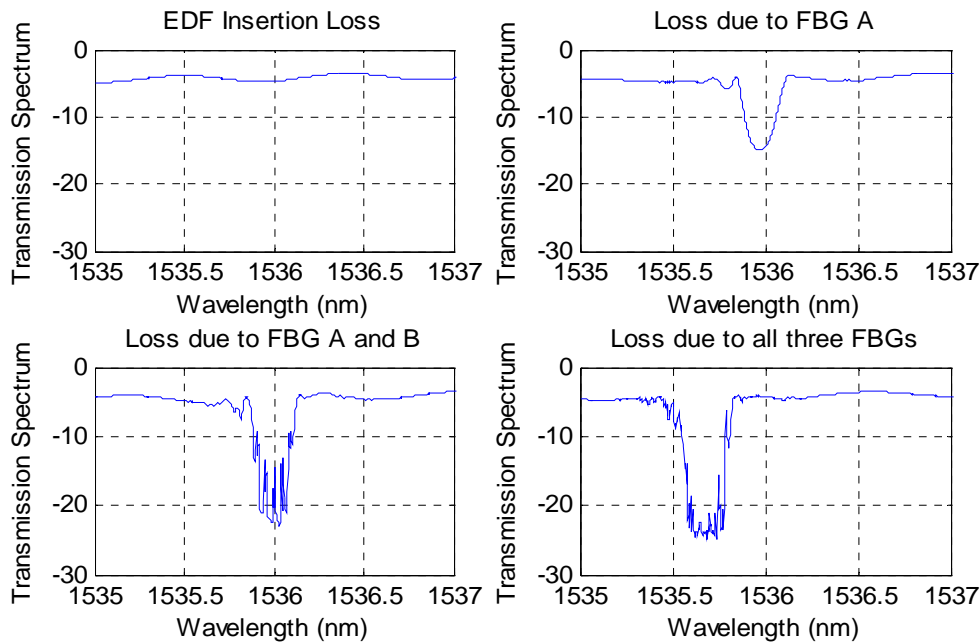


Fig. 7. Transmission spectrum of a 2 cm/ 8 cm CCFL at various stages of fabrication.

4.2. Spectral Characterization

Fig. 8(a) shows the lasing spectra of the CCFL pumped with a 980 nm laser diode at 40 mW. The pump was connected in through the 3 cm cavity end and the lasing spectrum is measured from the 9 cm cavity end using an optical spectrum analyzer (OSA) with a resolution of 0.06 nm. Fig. 8(b) compares the measured mode shape of the CCFL with that of a DFB fiber laser fabricated with 3 cm of the same type of EDF. Both lasers were pumped with a 980 nm laser diode at 85 mW and measured using a Fabry Perot tunable filter (FPTF). The experimental setup used for the results illustrated in Fig. 8(a) and 8(b) is also similar to the setup used in the following section as indicated in Fig. 9(a). Upon comparison with the DFB fiber laser, which operates inherently in a single longitudinal mode, it may be verified that the CCFL is also single-mode. Also, due to its much longer cavity length, the peak intensity of the CCFL was 6dB higher than the DFB fiber laser. In this context, long cavity length CCFLs may be considered to be more efficient in general than DBR or DFB fiber lasers with shorter cavity lengths.

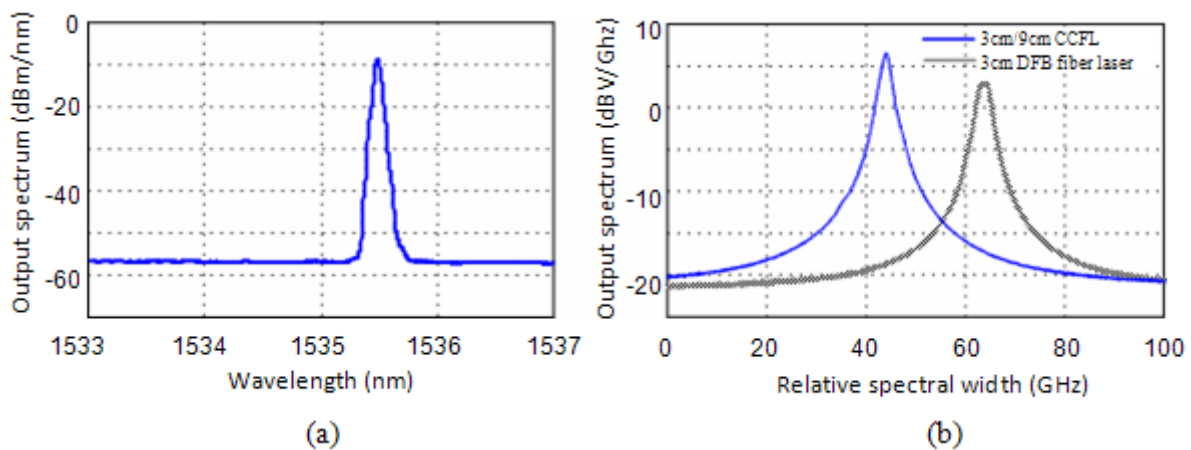


Fig. 8. Lasing spectra of the CCFL (a) measured using an optical spectrum analyzer; (b) compared to a DFB fiber laser measured using Fabry Perot tunable filter.

5. Experiment for the Three Straining Formats

The experiment setup used to operate the CCFL, and to detect the wavelength shift for the 3 straining formats is shown in Fig. 9(a). The 980 nm pump wavelength is channeled to the CCFL via a wavelength division multiplexer (WDM) and 10m in length of downlead fiber. The downlead fiber used is a StockerYale fiber with a single mode cut-off at 890 to 950 nm, and a mode field diameter of approximately 10 μm at 1550 nm. The WDM also serves to channel the returning CCFL emission (which does not contain any residual pump wavelength) to a FPTF. An isolator is placed between the WDM and FPTF to prevent undesirable back reflections into the CCFL. An OSA is connected to the forward emission, to monitor the general status of the CCFL. 30 mW of pump power was applied to the CCFL, which produced an emission at 1535 nm. A continuous ramp voltage is applied to the FPTF to detect the minute changes in lasing frequency of the CCFL. Due to the wavelength ambiguity introduced by the FPTF, the results will be expressed in terms of relative frequency shift. The spectral width of the FPTF is approximately 1.75 GHz (~ 14 pm), and at 1535 nm, a 1nm shift in wavelength is equivalent to a relative frequency shift of approximately 127 GHz.

The test method for the three straining formats is illustrated in Fig. 9(b). For each straining format, an upper gluing point is used to secure the CCFL against a floating shelf, so that it is hung vertically. A lower gluing point is then used to secure a light weight container. Calibrated weights are placed in the container to control the strain applied to the section of the CCFL between the two gluing points. To ensure consistency in the results, the same (3 cm, 9 cm) CCFL was used throughout the experiments Acetone was used to dissolve the glue after each set of measurements. To maintain the original spectral response, care was taken to ensure that the glue was not applied on the three FBGs which would cause a spectral mismatch of the gratings. After the glue had cured, measurements showed that only 8 mm of the 3 cm cavity (27 % of cavity length) and 64mm of the 9 cm cavity (71 % of cavity length) were prone to the longitudinal strain, resulting only 27 % of potential sensitivity is utilized for the 3 cm cavity and 71 % for the 9 cm cavity.

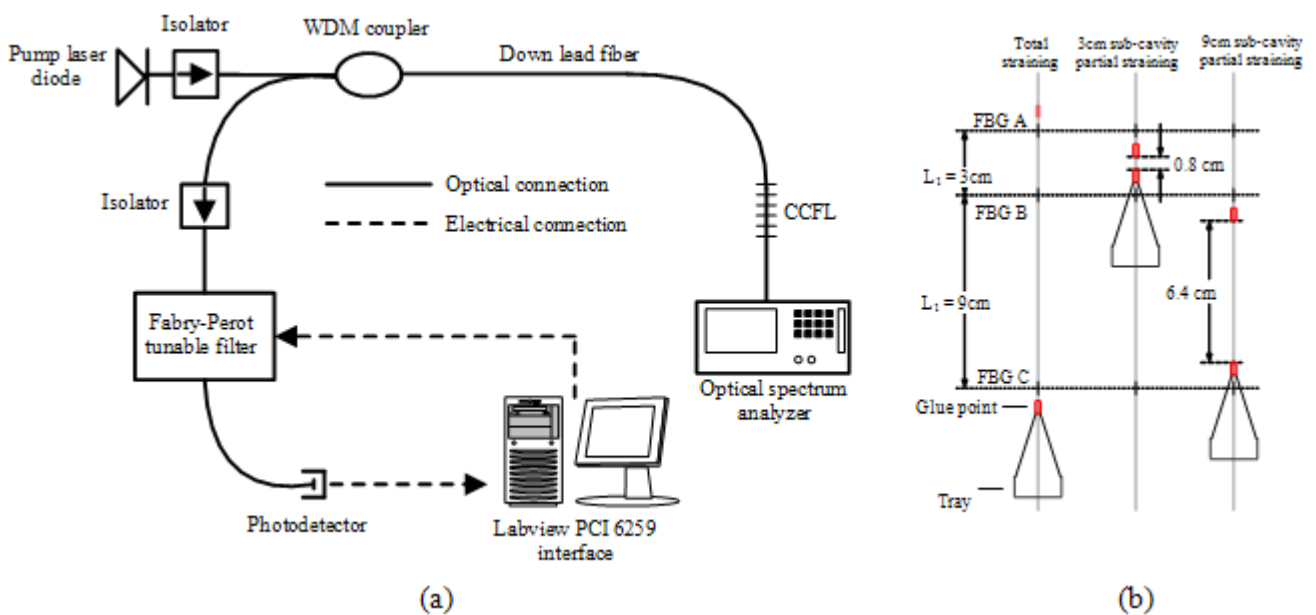


Fig. 9. (a) Experimental setup used to test the CCFL under various straining formats; and (b) setup to reproduce each straining format.

5.1. Experiment Results

The relative frequency shifts of the CCFL under the three sensing formats are shown in Fig. 10 to 12. In these figures, measurements whose lasing peaks were found to be off-trend are plotted as circles. The likely cause of the instability is the twisting of the laser cavity (between the two gluing points) as the weights were added into the container. For the total cavity straining format shown in Fig. 10, a linear 1.16 pm/ $\mu\epsilon$ response was observed, which was intuitively and theoretically expected. For the 3 cm sub-cavity straining format shown in Fig. 11, the response appears to be separated into four segments, caused by the longitudinal modes moving in and out of the spectral width of the FBGs, i.e. four lasing modes had scanned through the FBG's spectral width over 170 $\mu\epsilon$. The average response of the four mostly-linear segments is approximately 0.47 pm/ $\mu\epsilon$, which is lower than that of the total cavity straining format (referring to Fig. 5) since only 27 % cavity is prone to the strain. If the full 3 cm was utilized, then these results would predict a response of 1.7 pm/ $\mu\epsilon$, 40 % in excess of that of the linear response. As expected for the 9 cm sub-cavity straining format shown in Fig. 12, the lasing wavelength was much less sensitive to strain. Due to feedback and self-injection, the free spectral range of the 3 cm sub-cavity is the dominant effect in determining the lasing frequency and so the wavelength response from straining the 9 cm cavity would not be as noticeable. The oscillating wavelength response that was observed in the simulated results of Fig. 5 could not be substantiated from the experimental results of the partial straining formats. From measurements obtained during the fabrication of the 3 cm/ 9 cm CCFL, each of the 6mm gratings had about 10 dB transmission loss ($r_C \approx 0.95$) at the Bragg wavelength. Using an estimated linear net gain of a fiber laser of low pump power (40 mW) as 1 m^{-1} , the calculated round trip gain, g_2 is less than 1.2. The resulting $r_C g_2$ is a rather non-optimized value, which possibly reduces the magnitude of the wavelength sensitivity according to Fig. 6. While it is not possible to demonstrate the predicted sensitivity increase in the current case as discussed above, the experimental results illustrated in Fig. 10 to 12 have shown the nonlinear response and the differences in spectral requirements. For the total cavity sensing format, although it is the simplest to operate, the spectral allocation required is proportional to the dynamic range of the sensor. Conversely, for the two partial cavity sensing formats, the allocations required are mostly determined by the spectral width of the FBGs. If fringe counting or similar techniques are applied in conjunction with the short sub-cavity sensing format, the number of sensors that can be multiplexed is vastly increased, but one should take into account the nonlinear behavior of the CCFL in this case.

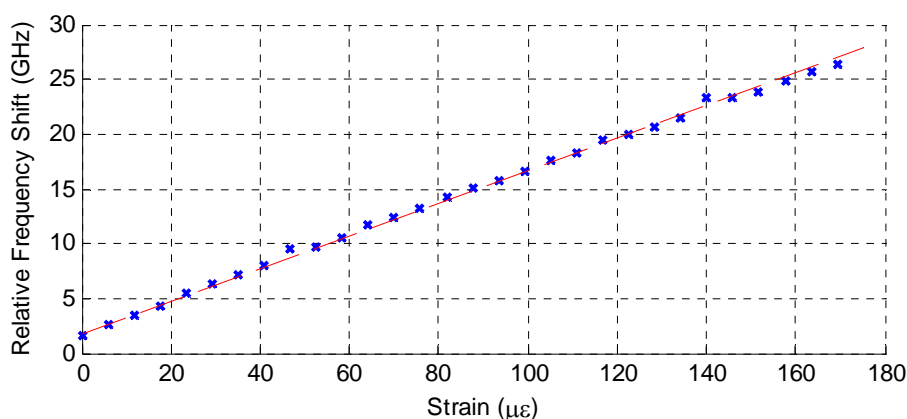


Fig. 10. Linear response observed from total CCFL straining.

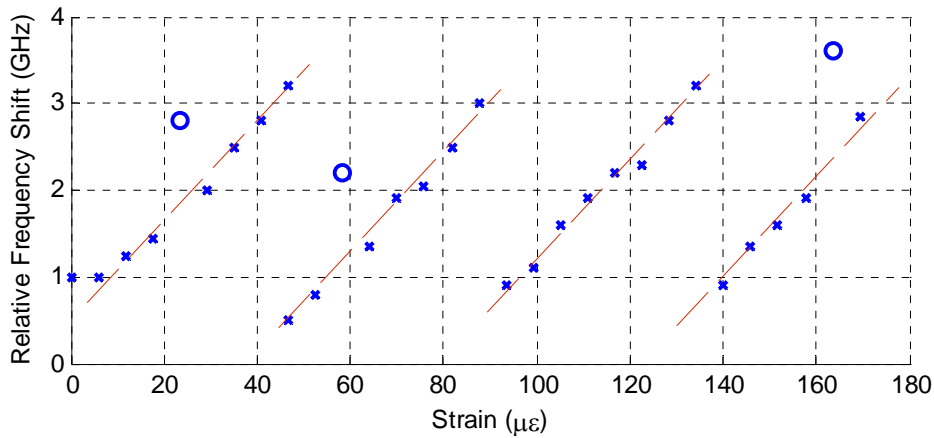


Fig. 11. Response observed from partial CCFL straining of the 3cm sub-cavity.

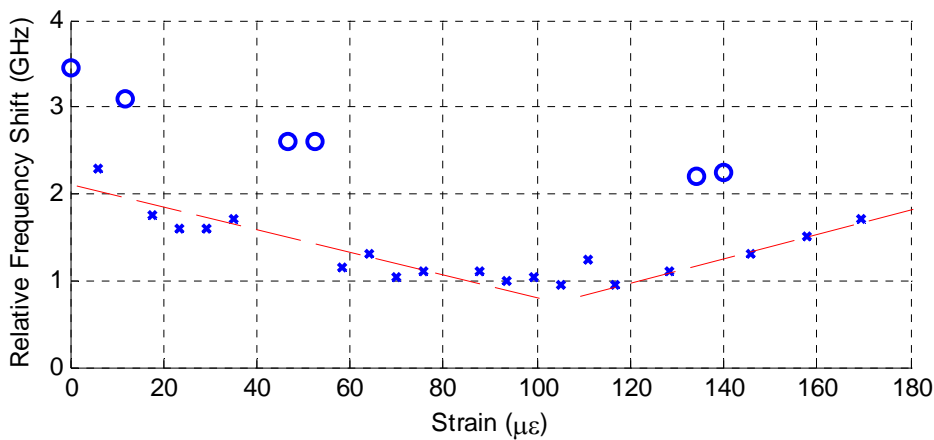


Fig. 12. Response observed from partial CCFL straining of the 9cm sub-cavity.

6. Conclusion

Composite cavity fiber laser (CCFL) was examined theoretically and experimentally for their potential use in sensing. An in house fabricated CCFL with dimension (3 cm, 9 cm) was fabricated, characterized and experimented. A simple straining experiment was carried out to investigate different sensing formats of the CCFL. The preliminary results agree with theoretical expectations. The strain response of the CCFL is the same as that of a FBG or single cavity fiber laser sensor when the cavity was totally utilized for straining. The responses can be significantly different for the case of partial straining of the sub-cavity, with alternating sections of higher and lower wavelength sensitivity and differences in spectral requirements. CCFL sensor demonstrates promising performance with the increased sensitivity and narrow spectral allocations shown by primary (3cm) partial cavity sensing format. Deployment of CCFL into specific application may be required further investigation due to the stringent requirements of particular application.

References

- [1]. G. A. Cranch, G. Flockhart, C. K Kirkendall. Distributed feedback fiber laser strain sensors, *IEEE Sensors J.*, Vol. 8, No. 7, 2008, pp. 1161-1172.

- [2]. S. Foster, A. Tikhomirov, M. Milnes, J. Van Velzen, J. G. Hardy. A fibre laser hydrophone, in *SPIE Proceedings of the 17th International Conference on Optical Fiber Sensors*, Bellingham, USA, 23 May 2005, Vol. 5855, pp. 627-630.
- [3]. O. Haderer, E. Ronnekleiv, M. Ibsen, R. I. Laming. Polarimetric distributed feedback fiber laser sensor for simultaneous strain and temperature measurements, *Appl. Opt.*, Vol. 38, No. 10, pp. 1953-1958.
- [4]. J. Mandal, S. Tong, K. T. V. Grattan, Z. Rui Tao, N. Nam Quoc, A. T. Augousti. A parallel multiplexed temperature sensor system using Bragg-grating-based fiber lasers, *IEEE Sensors J.*, Vol. 6, No. 4, 2006, pp. 986-995.
- [5]. K. Liu, W. Jing, G. D. Peng, J. Zhang, Y. Wang, T. Liu, D. Jia, H. Zhang, Y. Zhang. Wavelength sweep of intracavity fiber laser for low concentration gas detection, *IEEE Photonics Technol. Lett.*, Vol. 20, No 18, 2008, pp. 1515-1517.
- [6]. G. Whitenett, G. Stewart, Y. Hongbo, B. Culshaw. Investigation of a tuneable mode-locked fiber laser for application to multipoint gas spectroscopy, *IEEE J. Lightwave Technol.*, Vol. 22, No. 3, 2008, pp. 813-819.
- [7]. S. M. Melle, A. T. Alavie, S. Karr, T. Coroy, K. Liu, R. M. Measures, A Bragg grating-tuned fiber laser strain sensor system, *IEEE Photonics Technol. Lett.*, Vol. 5, No. 2, 1993, pp. 263-266.
- [8]. Y. O. Barmenkov, A. Ortigosa-Blanch, A. Diez, J. L. Cruz, M. V. Andres, Time-domain fiber laser hydrogen sensor, *Opt. Lett.*, Vol. 29, No. 21, 2004, pp. 2461-2463.
- [9]. S. Goodman, A. Tikhomirov, S. Foster, Pressure compensated distributed feedback fibre laser hydrophone, in *SPIE Proceedings of the 19th International Conference on Optical Fiber Sensors*, Perth, Australia, 14 April 2008, Vol. 7004, pp. 700426-700426.4.
- [10]. A. Tikhomirov, S. Foster, DFB FL sensor cross-coupling reduction, *IEEE J. Lightwave Technol.*, Vol. 25, No. 2, 2007, pp. 533-538.
- [11]. C. K. Kirkendall, A. Dandridge, Overview of high performance fibre-optic sensing, *J. Phys. D: Appl. Phys.*, Vol. 37, No. 18, 2004, pp. 197-216.
- [12]. N. Schunk, K. Petermann, Numerical analysis of the feedback regimes for a single-mode semiconductor laser with external feedback, *IEEE J. Quantum Electron.*, Vol. 24, No. 7, 1988, pp. 1242-1247.
- [13]. S. Saito, Y. Yamamoto, Direct observation of Lorentzian lineshape of semiconductor laser and linewidth reduction with external grating feedback, *Electron. Lett.*, Vol. 17, No. 9, 1981, pp. 325-327.
- [14]. L. Goldberg, A. Dandridge, R. O. Miles, T. G. Giallorenzi, J. F. Weller, Noise characteristics in line-narrowed semiconductor lasers with optical feedback, *Electron. Lett.*, Vol. 17, No. 19, 1981, pp. 677-678.
- [15]. R. Wyatt, W. J. Devlin, 10 kHz linewidth 1.5 μm InGaAsP external cavity laser with 55 nm tuning range, *Electron. Lett.*, Vol. 19, No. 3, 1983, pp. 110-112.
- [16]. D. Mehuys, M. Mittelstein, A. Yariv, Optimised Fabry-Perot (AlGa)As quantum-well lasers tunable over 105 nm, *Electron. Lett.*, Vol. 25, No. 2, 1989, pp. 143-145.
- [17]. A. Olsson, C. Tang, Coherent optical interference effects in external-cavity semiconductor lasers, *IEEE J. Quantum Electron.*, Vol. 17, No. 8, 1981, pp. 1320-1323.
- [18]. J. Osmundsen, N. Gade, Influence of optical feedback on laser frequency spectrum and threshold conditions, *IEEE J. Quantum Electron.*, Vol. 19, No. 3, 1983, pp. 465-469.
- [19]. I. Leung, A. C. L. Wong, G. D. Peng, Strain related characteristics of composite cavity fiber lasers, in *SPIE Proceedings of the Advanced Sensor Systems and Applications*, Beijing China, 26 November 2007, Vol. 6830, pp. 68301W-68301W-9.
- [20]. J. Roths, F. Julich, Determination of strain sensitivity of free fiber Bragg gratings, in *SPIE Proceedings of the Optical Sensors*, Strasbourg, France, 6 June 2008, Vol. 7003, pp. 700308-700308-8.

Guide for Contributors

Aims and Scope

Sensors & Transducers Journal (ISSN 1726-5479) provides an advanced forum for the science and technology of physical, chemical sensors and biosensors. It publishes state-of-the-art reviews, regular research and application specific papers, short notes, letters to Editor and sensors related books reviews as well as academic, practical and commercial information of interest to its readership. Because it is an open access, peer review international journal, papers rapidly published in *Sensors & Transducers Journal* will receive a very high publicity. The journal is published monthly as twelve issues per annual by International Frequency Association (IFSA). In addition, some special sponsored and conference issues published annually. *Sensors & Transducers Journal* is indexed and abstracted very quickly by Chemical Abstracts, IndexCopernicus Journals Master List, Open J-Gate, Google Scholar, etc.

Topics Covered

Contributions are invited on all aspects of research, development and application of the science and technology of sensors, transducers and sensor instrumentations. Topics include, but are not restricted to:

- Physical, chemical and biosensors;
- Digital, frequency, period, duty-cycle, time interval, PWM, pulse number output sensors and transducers;
- Theory, principles, effects, design, standardization and modeling;
- Smart sensors and systems;
- Sensor instrumentation;
- Virtual instruments;
- Sensors interfaces, buses and networks;
- Signal processing;
- Frequency (period, duty-cycle)-to-digital converters, ADC;
- Technologies and materials;
- Nanosensors;
- Microsystems;
- Applications.

Submission of papers

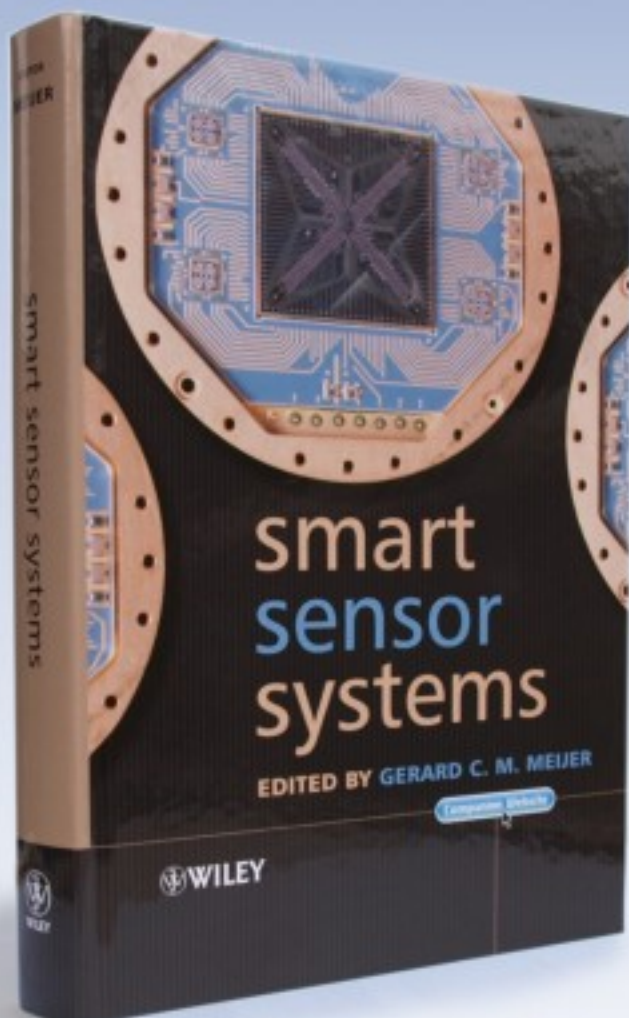
Articles should be written in English. Authors are invited to submit by e-mail editor@sensorsportal.com 8-14 pages article (including abstract, illustrations (color or grayscale), photos and references) in both: MS Word (doc) and Acrobat (pdf) formats. Detailed preparation instructions, paper example and template of manuscript are available from the journal's webpage: <http://www.sensorsportal.com/HTML/DIGEST/Submission.htm> Authors must follow the instructions strictly when submitting their manuscripts.

Advertising Information

Advertising orders and enquires may be sent to sales@sensorsportal.com Please download also our media kit: http://www.sensorsportal.com/DOWNLOADS/Media_Kit_2009.pdf

 **WILEY**
1807-2007

KNOWLEDGE FOR GENERATIONS



'Written by an internationally-recognized team of experts, this book reviews recent developments in the field of smart sensors systems, providing complete coverage of all important systems aspects. It takes a multidisciplinary approach to the understanding, design and use of smart sensor systems, their building blocks and methods of signal processing.'



Order online:

http://www.sensorsportal.com/HTML/BOOKSTORE/Smart_Sensor_Systems.htm

www.sensorsportal.com